Identifying acoustical coupling by measurements and prediction-models for St. Peter's Basilica in Rome

Francesco Martellotta
Dipartimento di Architettura e Urbanistica, Politecnico di Bari, via Orabona 4, 70125 Bari, Italy

(Received 27 May 2009; revised 3 July 2009; accepted 6 July 2009)

St. Peter's Basilica is one of the largest buildings in the world, having a huge volume resulting from the addition of different parts. Consequently, sound propagation cannot be interpreted using a conventional approach and requires experimental measures to be compared with statistical-acoustics and geometrical predictions in order to explain the interplay between shape, materials, and sound waves better. In previous research one of the most evident effects, the surprisingly low reverberation time, was believed to result from acoustical coupling phenomena. Taking advantage of more refined measuring techniques available today an acoustic survey was carried out and the results were analyzed using different methods, including Bayesian parameter estimation of multiple slope decays and directional energy plots, which showed that coupling effects actually take place, even though measured reverberation times were longer than those given in previous studies. In addition, experimental results were compared with geometrical- and statistical-acoustic models of the basilica, which showed that careful selection of input data and, in statistical models, the inclusion of phenomena such as direct sound radiation and non-diffuse energy transfer, allow obtaining accurate results. Finally, both models demonstrated that reduced reverberation depends more on increased absorption of decorated surfaces than on coupling effects.
 [DOI: 10.1121/1.3192346]

PACS number(s): 43.55.Br, 43.55.Gx [NX] Pages: 1175–1186

I. INTRODUCTION

Large reverberant spaces are frequently encountered in acoustical practice. Concert halls, auditoriums, and theaters may have volumes of tenths of thousands m^3, but the way the sound propagates inside them is well understood, provided that their shapes are reasonably proportionate.[1,2] Larger enclosed spaces are much less frequently found and, consequently, their acoustic properties are less investigated. Churches represent an important example of very large (and sometimes huge) buildings whose acoustic characteristics have been investigated since the early stages of acoustic science.[3,4] However, churches are not only large but, due to historical and architectural reasons, they also are complex, resulting from the combination of multiple volumes, which make sound propagation even more difficult to understand. In fact, large volumes are expected to be very reverberant, but the presence of richly decorated surfaces scattering the sound, combined with architectural complexity, mostly related to the presence of aisles, domes, or chapels, may sometimes contradict this simple expectation.

A remarkable example of this unusual behavior is St. Peter's Basilica in Rome, characterized by its huge volume of 480 000 m^3. In the early 1970s Shankland and Shankland[5] measured reverberation time in St. Peter's Basilica by means of a tape recorder and by ear and stopwatch. The results they obtained, although biased by the "subjective" approach, were quite surprising as they estimated a mid-frequency reverberation time of 7.1 s, a value lower than those observed in other smaller churches.[4–6] The authors explained this unexpected result as being the consequence of the weak acoustic coupling between the different parts of the church, a hypothesis that was later also used to explain similar discrepancies in Greek Byzantine churches.[7] Measurements carried out 20 years before, but with more refined techniques, in the basilicas of St. John Lateran and St. Paul outside the Walls in Rome[4] pointed out the existence of coupling phenomena in the first church, where different parts are connected by means of small apertures, also emphasizing (by comparing the two churches) the importance of sculptures and decorations in reducing the reverberation time. Measurements carried out in another of the largest worship buildings, St. Paul's Cathedral in London,[8] showed that despite its smaller dimensions (152 000 m^3) the measured reverberation time in unoccupied conditions is about 10.5 s. Later studies[9] showed, using a mathematical model, that coupling effects also take place in this church, confirming that the relationship between reverberation and coupling is not obvious and requires detailed investigation.

Even though the theoretical foundations of acoustic coupling were clearly stated by several researchers,[1,2,10] initially the identification of such phenomena from measured decay traces could only be made (in the best cases) by visual inspection.[4] Later on, the use of decay curves obtained from backward integrated impulse responses (IRs) (Schroeder plots) provided more detailed data, which, nonetheless, could hardly give reliable quantitative measures of the different decay rates. Concepts such as the "running reverberation"[9] or ratios between different portions of the reverberant decay[11] were used to describe the slope variation as a function of time. It was only the introduction of Bayesian parameter estimation[12–15] that opened up new perspectives in the research on acoustic coupling. In fact, in this way, a rigorous estimate of the different decay constants that characterize

multi-rate decay processes is possible, also allowing more accurate comparisons with theoretical models.

From this point of view the original two-room model[1] based on statistical-acoustics (SA) assumptions was first extended (by means of matrix notation) to a larger number of sub-rooms[2] and, more recently, the model was further generalized[16] by including a number of effects (such as direct sound radiation and non-diffuse transfer of energy), which allowed even more accurate analysis of the sound propagation in complex coupled systems. In addition, advancements in the geometrical-acoustic (GA) modeling[17] allowed improved prediction accuracy when using beam-axis/ray-tracing algorithms.

Taking advantage of the much more accurate measuring methods available today, allowing for three-dimensional (3D) sound field decomposition, flat frequency response, and high signal-to-noise ratios,[18] together with the possibility of better investigating coupling effects by means of Bayesian estimation, and to use these data to validate SA or GA models, a new survey was carried out in St. Peter's Basilica in order to analyze and distinguish the proportionate effects of surface absorption and acoustical coupling on reverberation.

II. THE ACOUSTIC SURVEY

A. Description of the church

The building of St. Peter's Basilica started in 1506, on the same site where the old Constantinian basilica had been built, in order to preserve the coincidence between the altar position and the tomb of the saint. The first architect appointed for the design of the new church was Bramante. After his death many others succeeded, but the current shape and the dome design were mostly due to Michelangelo's work, which started in 1547. The basilica was finally consecrated in 1626 after Carlo Maderno had modified Michelangelo's plans by adding the long nave (Fig. 1). Decorative works went on for several years. The basilica may be considered as the sum of five large volumes (the three braces of the original Greek cross, the main nave, and the domed crossing), joined together by means of the large openings of the crossing and by means of additional secondary volumes connected through smaller openings.

Its huge dimensions are characterized by a total length of 185 m, a nave width of about 26 m, a dome width of 41.5 m, and height (up to the lantern) of about 120 m. The resulting volume of the basilica, calculated by means of a computerized 3D model, is about 480 000 m^3, and the total surface area (assuming all the surfaces as flat) is about 80 000 m^2, 12 600 m^2 of which corresponds to the usable floor surface. Most of the surfaces are finished in plaster, marble, or stucco, but they are richly decorated with deep carvings (Fig. 2). The area of glazed surfaces is approximately 2000 m^2. Pews (with upholstered kneelers) are only installed in the choir, while the remaining floor areas are completely bare. At the center of the main nave a wooden barrier is installed to protect the central part of the floor.

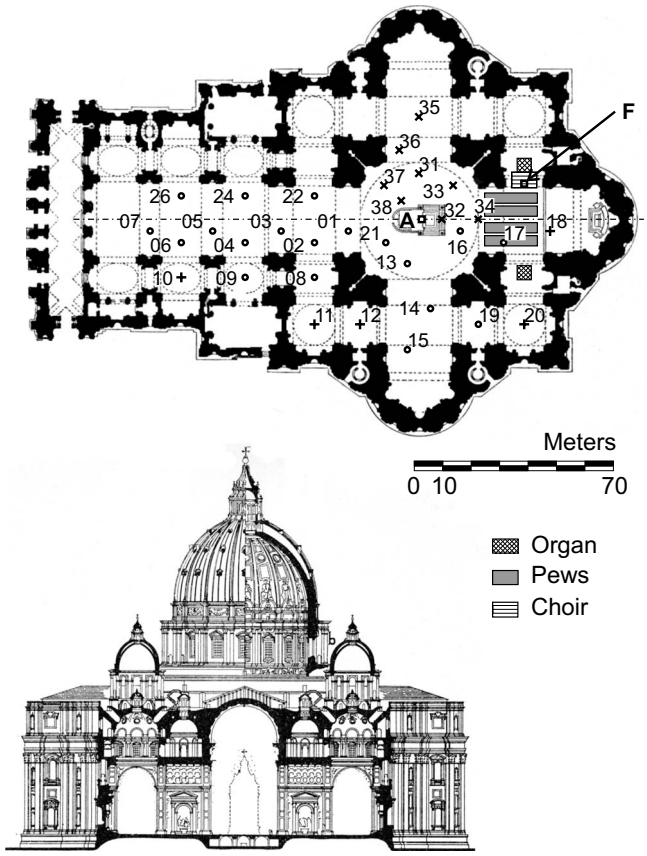

FIG. 1. Plan and section of the basilica, with indication of the source (A and F) and receiver (1–39) locations. (○) B-format microphone, (+) omnidirectional microphone, and (×) omni+figure-of-eight microphone.

B. Measurement techniques

Measurements were carried out in unoccupied conditions, during daytime between 9.00 and 10.30, just before the Wednesday Mass in St. Peter's Square. About 30 people (mostly security officers, priests, and other workers) could not leave the basilica during the measurements, but they were asked to perform only "silent" tasks in order to avoid interferences. Indoor air temperature was 21 °C, relative humidity was 60%, and both values remained constant during the measuring session. Measurements were carried out com-

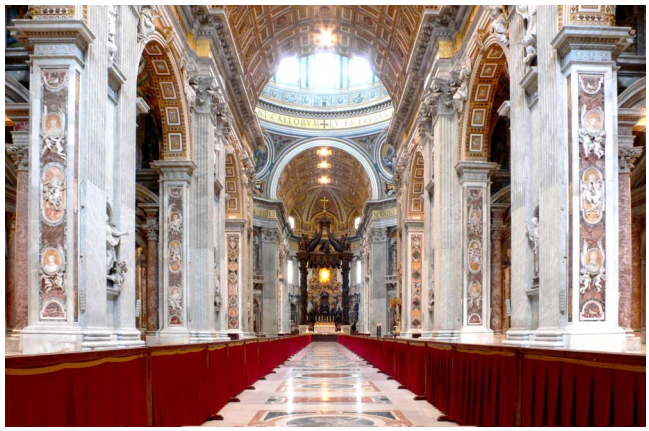

FIG. 2. (Color online) View of the interior of the church taken from the main entrance.

plying with ISO 3382 standard[19] also taking into account a set of guidelines specifically defined for churches.[20] Given the building dimensions and strict time limitations, the measurements were carried out using a special set-up. Two omnidirectional sound sources (a Look-Line D301 and a self-made dodecahedron made of twelve 120 mm loudspeakers), each one combined with an additional sub-woofer to cover low frequencies, were located, respectively, 2 m in front of the altar (position A) and in front of the organ on the left ("in cornu evangeli," position F), where there are also choir stalls installed. Source A was located 1.5 m above the altar floor, which is about 1.5 m higher than the nave floor. Source F was located 1.5 m above the risers of the choir stalls. Each sound source was fed by a different constant-envelope equalized sine sweep (40 s long) generated using MATLAB according to Müller and Massarani[18] so that the spectrum of the radiated sound was substantially flat from the 50 Hz to the 16 kHz third-octave bands. High-quality IRs were collected by using three measurement chains. The first chain included a B-format microphone (Soundifield Mk-V) and a binaural head and torso (B&K 4100D) connected to an Echo Audio Layla 24 sound card. The second chain included a Neumann TLM-127 with variable polar pattern, allowing the measurement of both omni-directional and figure-of-eight IRs, connected to an Echo Audio Fire 8 sound card. The third chain included an omni-directional microphone (GRAS 40-AR) connected to a portable digital audio tape recorder, used to get IRs in the farthest positions. In all the cases the room responses were recorded at a sampling rate of 48 kHz and 24 bit depth, to obtain, after deconvolution (performed using MATLAB), IRs with a signal-to-noise ratio, which even in the worst cases (receivers located more than 100 m from the source) allowed a "safe" calculation of reverberation time (T_{30}) based on at least 30 dB of decay even at the lowest frequencies. Globally, 33 receivers placed 1.2 m from the floor surface were distributed throughout the church according to the layout given in Fig. 1.

III. ANALYSIS OF EXPERIMENTAL RESULTS

A. Reverberation times

The analysis of experimental results started by taking into account conventional measures of T_{30} and early decay time (EDT) resulting from IRs measured in the locations distributed throughout the church in combination with both source positions (Fig. 1). The analysis of the average T_{30} as function of frequency (Fig. 3) shows the typical behavior observed in churches mostly finished in hard reflecting materials, characterized by long values at low frequencies (13.6 s) rapidly decreasing as the frequency grows due to air absorption, with a mid-frequency value of 9.9 s and a minimum of 2.2 s at 8 kHz. Average reverberation time is actually smaller than expected. In fact, given the huge volume, mid-frequency reverberation time should be well above 10 s (see, for example, St. Petronio Basilica in Bologna[6] having a volume of 170 000 m^3 and a mid-frequency T_{30} of 10.7 s). However, it is interesting to observe that measured values are longer than those reported in Ref. 5, especially at low frequencies.

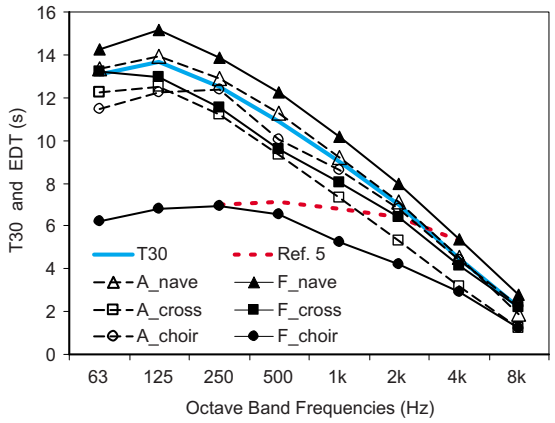

FIG. 3. (Color online) Octave-band values of average reverberation time (T_{30}) compared with measurements reported in Ref. 5, and EDT subdivided into different source and receiver locations.

Average EDT values as a function of frequency show negligible differences from T_{30}, being 0.2 s shorter at mid-frequencies. However, while standard deviation among measured T_{30} is very small (0.39 s at 1 kHz), the corresponding value for EDT is considerably larger (1.4 s at 1 kHz), suggesting a possible relationship with source placement and, above all, with source-receiver distance. When the source was in front of the altar (A) the average EDT values measured in the nave closely followed T_{30} behavior, while average EDT measured in the choir and in the crossing (the central volume where the braces converge) was slightly lower. The largest variations appeared when the source was located in the choir, showing average EDT values measured in the same subspace to be much lower (mid-frequency value being 5.9 s) than in the crossing (8.8 s), and in the nave (11.2 s). The latter were the largest values observed during the survey, being larger than those measured at the same receivers when the source was at A (10.2 s).

Given the measurement procedure used by Shankland and Shankland,[5] their reverberation times were expected to be more similar to EDT values (Fig. 3). However, apart from a better agreement at 1 and 2 kHz, moving toward low frequencies, no such relationship appears although the description of the measurement conditions seems substantially similar (no pews on the floor and no occupancy), and no significant changes have been made to the building since that survey. The discrepancy might be the result of different source placements, as values given in Ref. 5 correspond to both source and receivers in the nave, but they also give values measured in the crossing, and the small increase of just 0.2 s is well below the values measured in the present survey in the same conditions. So, it may be reasonably supposed that the "ear and stopwatch" method used in the measurements of the 1970s failed, especially at low frequencies, in such a huge volume where reaching adequate sound levels to measure T_{30} is a challenge even for today's instruments.

B. Analysis of spatial variations

A more detailed analysis of the nature of EDT differences was obtained by plotting mid-frequency T_{30} and EDT values as a function of source-receiver distance (Fig. 4). It

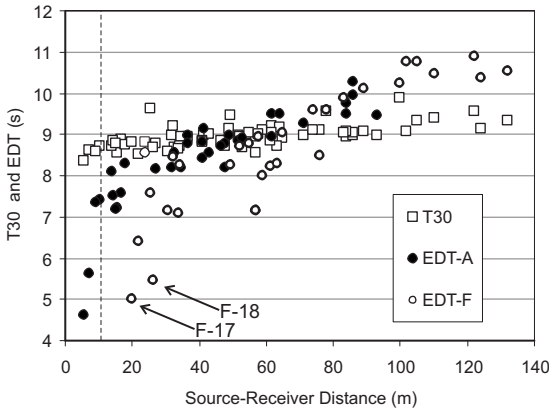

FIG. 4. Plot of T_{30} and EDT values at 1 kHz octave band, as a function of source-receiver distance. EDT values are further divided as a function of source placement.

can be observed that T_{30} shows only a mild increasing trend (with a slope of 0.7 s/100 m), while EDT shows a substantially different behavior, with a much steeper increase as a function of the distance, and a further dependence on the sound source location.

In fact, an increase in EDT as a function of distance is typically observed in churches as a consequence of the weak direct sound and early reflections arriving at the farthest points, which slow the transition toward the purely exponential decay of the diffuse sound energy.[21,22] However, in this case, two different trends appear, with a steeper slope when the source was in the choir (4.8 s/100 m) compared to the value observed when the source was in the crossing (2.7 s/100 m). Such a difference may depend on the larger number of obstacles that sound coming from the choir encounters during its propagation, affecting direct sound and early reflections. However, when both source and receiver are in the choir (and the direct sound path is unobstructed), EDT is markedly lower than at similar (equally unobstructed) combinations located in the crossing. This might well depend on early reflections differences, but a comparison of early decay traces (Fig. 5) shows that when both source and receiver are in the choir the initial part of the decay shows a long (about 8 dB) and markedly steeper slope. This provides evidence that EDT differences in the choir are not simply due to the

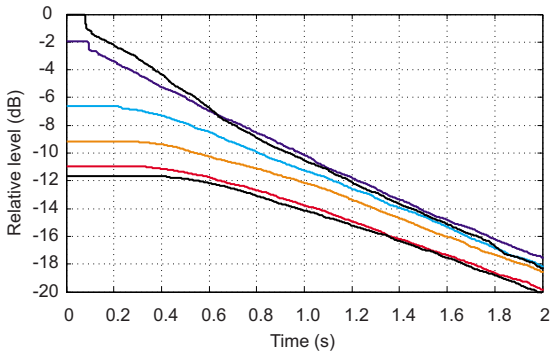

FIG. 5. (Color online) Plot of the early level decay for different receivers when the source is in the choir. Curves from top to bottom correspond to receivers 17, 21, 01, 03, 05, and 07. The topmost curve, corresponding to receiver 17, has a markedly different initial decay.

TABLE I. Summary of the results of Bayesian search of double slopes in measured IR.

S-R combination	E_{21} (dB)	$10\log(A_1/A_2)$ (dB)	T_1 (s)	τ_1 (s)	T_2 (s)	τ_2 (s)
F-17	97.0	1.0	3.2	0.044	8.9	0.151
F-18	133.6	3.2	3.3	0.058	8.9	0.108
F-34	105	−0.5	4.0	0.158	9.1	0.159
A-33	71.9	−5.0	1.3	0.071	8.4	0.071
A-21	68.0	−7.5	1.1	0.040	8.7	0.036
A-37	107.0	−3.0	0.8	0.025	8.3	0.051
A-38	66.3	−3.5	1.4	0.048	8.4	0.105

structure of early reflections but rather depend on diffuse-field variations between the given subspace and those to which it is connected.

C. Bayesian analysis

In order to investigate this hypothesis better, Bayesian analysis[12–15] provides a powerful and reliable tool to detect and quantify multiple slopes in IRs. Bayesian analysis is the most rigorous instrument for detecting double slopes in measured IRs and, hence, for investigating coupled-volume problems. The algorithm proposed by Xiang and Jasa[15] was implemented in MATLAB and several IRs were processed. Even though the procedure may be applied to a virtually unlimited number of decays, for the IR under test only double slopes gave the highest accuracy, evaluated by means of the Bayesian evidence E_{21}, as defined in Ref. 13. In order to create double slopes the best situation is when source and receiver are located in a subspace, which is less reverberant than the whole church. Consequently, source-receiver combinations located in the choir and in the crossing were investigated. Under these conditions the first (and shortest) decay (T_1) corresponds to the decay time of the subspace in which the source is located, while the second (T_2) corresponds to the coupled-system decay time. The relative amplitude of the two decays is evaluated by means of their logarithmic ratio as decay level difference. Finally, in order to estimate the accuracy of the decay time estimation, the procedure reported in Ref. 14 was followed, by calculating for each decay time the corresponding standard derivations (τ).

The following results are referred to the 1 kHz octave band (Table I), but similar results can be obtained at different bands. The highest estimation accuracy was obtained for combinations F-17 and F-18 (i.e., with both the source and receiver in the choir), providing a T_1 of 3.2 s and a T_2 of 8.9 s, in good agreement with the mean T_{30} value [Fig. 6(a)]. Standard derivation is small for the first decay (about 0.05 s) and somewhat longer for the second (about 0.13 s) but in both cases correspond to a 1.5% of the calculated value. Combination F-34 also showed a double slope, but its boundary position determined a T_1 of 4.1 s (with a standard derivation of 0.158 s) and a T_2 of 9.2 s. Results are less obvious out of the choir [Fig. 6(b)]. On average when the source and receivers were in the crossing T_1 was 1.3 s, while T_2 was 8.7 s. In all the cases the standard derivation is very small for both the decays. The first decay appears substan-

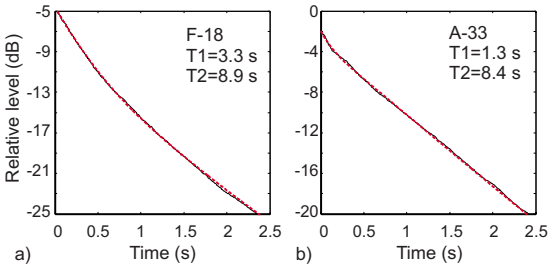

FIG. 6. (Color online) Comparison between measured decay (—) and multi-rate decay derived from Bayesian estimation (---) for combinations F-18 (a) and A-33 (b). Direct sound was excluded from each analysis.

tially shorter than in the choir, as a consequence of the wide openings. However, its magnitude is much smaller because of the large amount of acoustic energy flowing directly into adjacent sub-volumes. Consequently the coupled-system reverberation appears soon after the direct sound, resulting in EDT values generally longer than in the choir except at points very close to the source where the direct sound dominates. It is interesting to point out that even though Bayesian estimation shows that double decay rates take place, they barely affect T_{30}, confirming, as observed, that apart from a few cases the first decay expires soon.

D. Directional energy plots

The directional components of B-format measurements (X,Y,Z) were combined with the omni-directional component (W) to provide a 3D IR. Polar plots representing the energy content arriving from discrete directions represented by azimuthal and zenithal angles projected on the same plane were used to make the information more easily accessible. Then, also taking into account the time distribution, three time slices were considered: from 0 to 80 ms, from 80 to 200 ms, and from 200 to 1000 ms (Fig. 7). For each plot the level of the reflections was normalized assuming as a reference the maximum energy value for that slice.

A quantitative measure, which can be conveniently used in this analysis, is the directional diffusion δ as defined by Gover *et al.*,[23] so that a value equal to 0% corresponds to anechoic conditions, while 100% corresponds to perfectly diffuse sound field. In the present case δ was calculated with reference to the horizontal/azimuthal distribution (δ_h) and to the vertical/zenithal distribution (δ_v).

The analysis of combination F-17 [Fig. 7(a)] clearly shows that the first 80 ms are dominated by the direct sound and by few reflections in the horizontal plane, while in the vertical plane reflections appear weaker but quite diffuse. From 80 to 200 ms the dominance of the sub-volume is even clearer, with reflections mostly coming from the choir and very weak reflections coming from the crossing. From 200 to 1000 ms the reflections are more evenly distributed, but the dominant role of the choir is still evident as the reflections coming from the crossing are 5 dB weaker. This confirms that, as observed in Fig. 5(b), the coupled-system decay appears about 1 s after the direct sound.

It is interesting to observe, in comparison, the behavior of combination A-17 [Fig. 7(b)], which shows a clear dominance of the frontal reflections up to 200 ms, indicating that acoustic energy is mostly coming from the aperture, which connects the crossing, first in the form of direct sound and then as mostly diffuse reflections. In fact, from 200 to 1000 ms, diffuse reflections arrive from the choir side, providing the highest directional diffusion values.

Combination A-21 [Fig. 7(c)] is taken into account as an example of source and receiver located in the crossing, showing that within the first 80 ms the sound field is dominated by the direct sound and by reflections mostly located in the horizontal plane (in fact, the vertical distribution is quite oblong with important contributions coming from the floor). The directional diffusion is quite low, confirming that the large apertures prevent receivers located in this subspace from receiving strong early reflections. From 80 to 200 ms the reflections still come from the horizontal plane (mostly because of the high dome), and especially from the sides (identifiable as reflections from the pillars). From 200 to 1000 ms the sound field is more diffuse, but with a horizontal distribution, which suggests contributions from the choir and the transept, while reflections from the long nave are still lacking.

As a further comparison, it is useful to analyze combination A-05 [Fig. 7(d)], which shows a mostly frontal dominance up to 200 ms due to the combination of direct sound and diffuse energy arriving through the aperture. From 80 to 200 ms there are interesting contributions from the top, suggesting reflections from the barrel vaults. From 200 to 1000 ms reflections become more diffuse, but a clear axial dominance appears both in the horizontal and in the vertical plane suggesting a slow build-up of the purely reverberant field. Lack of strong lateral reflections may be explained as the result of the elongated geometry of the nave and of the wide and deep openings, which capture large amount of sound energy.

In conclusion the analysis of the directional energy plots allowed studying energy exchanges from a different perspective, giving information about which part of the room contributes to the decay at a given time.

IV. COMPARISON WITH THEORETICAL MODELS

A. Preliminary considerations

The above results only demonstrate that each subspace has its specific acoustic features, which influence the very beginning of the IR. In order to improve the knowledge of the coupling mechanism two parallel approaches were followed. First, a GA model was made using the CATT-ACOUSTIC V. 8.0h software, which implements a special algorithm to deal with coupled spaces.[17] Then, the generalized model of coupled subspaces proposed by Summers *et al.*[16] was applied.

However, both models share the definition of the space geometry and of surface characteristics. Room geometry was greatly simplified to take into account that geometric details that are small compared to wavelength are acoustically invisible or make the surface partly scattering (see Ref. 24, p. 176). Niches, sculptures, and decorations were replaced with simple flat surfaces having modified absorption and (only for GA) scattering properties. The need to modify absorption

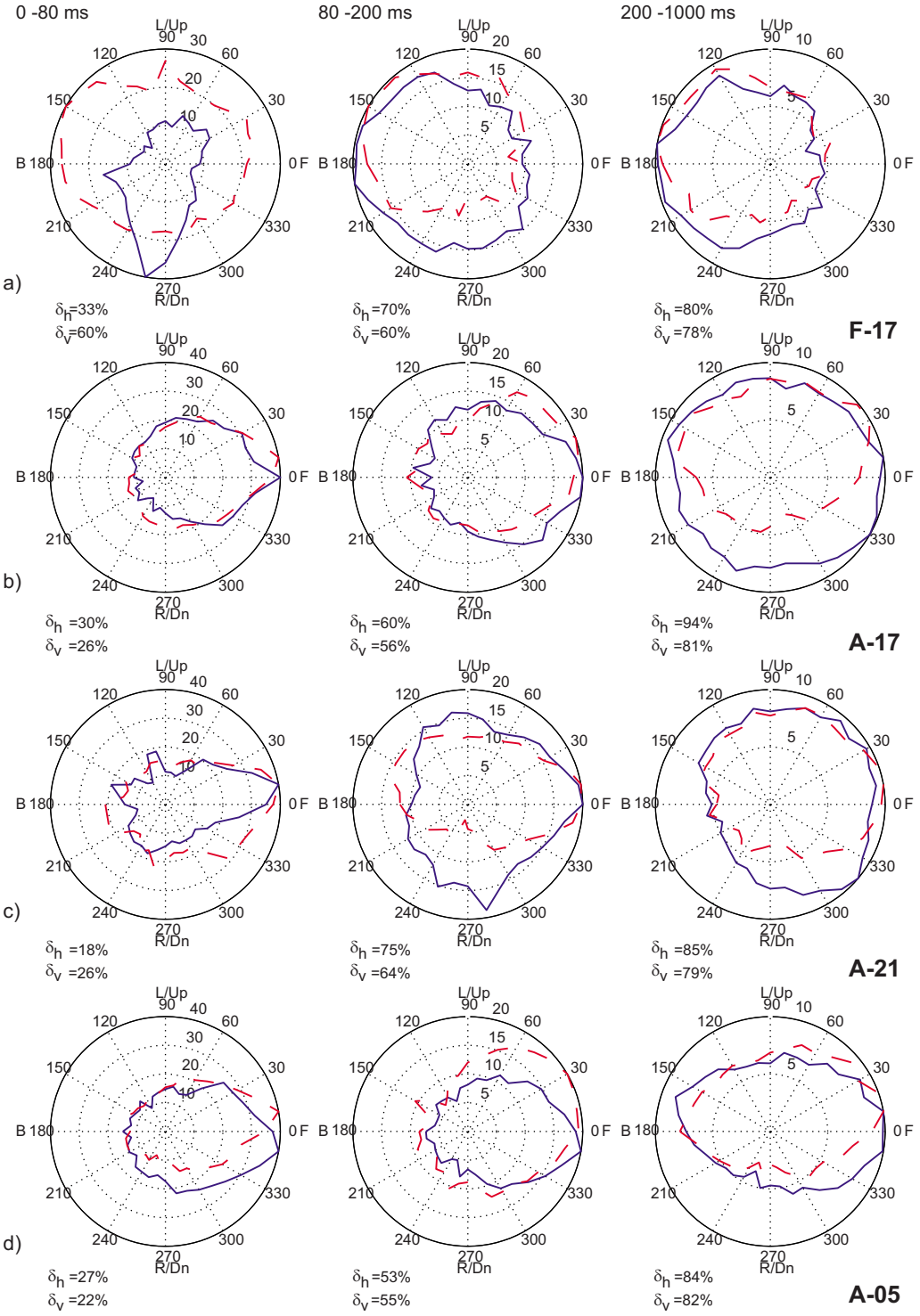

FIG. 7. (Color online) Polar plot of directional distribution of the energy content of the reflections at 1 kHz for different combinations of sources and receivers (F-17, A-17, A-21, and A-05). Reflection levels are normalized with reference to the maximum energy content for each time slice. (---) Energy level in the vertical plane and (—) energy level in the horizontal plane. Each receiver always points toward source A. δ_h=horizontal diffusion coefficient; δ_v=vertical diffusion coefficient; F=front, B=back, L/up=left/up, and R/Dn=right/down.

coefficients resulted from the increase in actual exposed area of decorated surfaces compared to the corresponding flat surface of the same material. Conversely, literature values[25,26] were assigned to pews, floors, glass, and wooden parts, which are normally assumed as flat (Table II). In order to better understand how conventional absorption coefficients had to be increased as a function of surface decorations further considerations were required.

Assuming Sabine's formula to be valid (neglecting coupling effects) the mean absorption coefficients (α) as a function of frequency, subtracting air absorption estimated using ISO 9613-1,[27] were calculated (Table III). However, taking into account that the flat floor surface is 12 600 m^2, the average absorption coefficient of the remaining surfaces is slightly higher, with a mid-frequency value of 0.10. Similar values are quite frequent in churches, especially when they

TABLE II. Summary of the absorption coefficients used in the GA and SA models.

	Fractional area (%)	Absorption coefficient per octave band (Hz)					
		125	250	500	1000	2000	4000
Marble floor (after Ref. 24)	17	0.01	0.01	0.2	0.02	0.03	0.03
Pews (after Ref. 24)	1	0.10	0.15	0.18	0.20	0.20	0.20
Glass (after Ref. 25)	3	0.35	0.25	0.18	0.12	0.07	0.04
Coffered vaults[a]	17	0.20	0.20	0.20	0.25	0.25	0.25
Dome and arches[a]	19	0.04	0.04	0.05	0.05	0.06	0.06
Sculptures[a]	3	0.12	0.12	0.15	0.15	0.18	0.18
Richly decorated marble/stuccos[b]	40	0.04	0.05	0.06	0.07	0.08	0.08

[a]Determined by comparison with similar surface treatments found in other churches.
[b]Determined from iterative calibration of GA model.

are richly decorated and characterized by a complex geometry, which determines large surface-to-volume ratio. The availability of a large set of acoustical and geometrical data[6] showed that over a sample of 56 different churches the minimum mid-frequency α (observed in seven churches) was 0.04, while the maximum was 0.14. The less absorbing group of churches was characterized by scarcely decorated plaster walls, hard stone floors (covered by few pews), and flat reflecting ceilings. The most absorbing group of churches was characterized by either richly decorated surfaces, coffered ceilings or large pew areas, or combinations of them. Taking into account the architectural features observed in the basilica, a mid-frequency α equal to 0.10 appears a perfectly suitable value.

However, assuming a uniform absorption on all the surfaces except the floor is not realistic as the decorative patterns are not evenly distributed. In fact, the exposed surface may be considerably different and, given the dimension of the church (and proportionally of the decorations, sometimes approaching half a meter in depth), the increased area is likely to be effective even at medium and low frequencies.

Comparisons between similar churches differing by just one element (provided it covered a reasonably large area) allowed estimation of the absorption coefficients of the given element. Thus, for a wooden coffered ceiling (like that found in the Cathedral of Taranto, or in the Basilica of Santa Maria Maggiore in Rome), α varies from 0.40 up to 0.60 at mid-frequencies, with small variations as a function of frequency. For a coffered dome finished in plaster (like that of the church of the Gran Madre di Dio in Turin) α varies between 0.20 at 125 Hz and 0.23 at 4 kHz. Finally, decorated surfaces, even though they are made of marble or plaster (like those found in the church of San Lorenzo in Turin, or in the church of San Luca e Martina in Rome), show a mid-frequency α varying between 0.08 and 0.10 according to the richness of the decorative pattern (and consequently of the exposed surface), while the variations as a function of frequency are relatively small. Taking into account these results it seemed that absorption coefficients should be increased over all the frequency bands including low frequencies. It is interesting to observe that this "wide-band" behavior and the increased absorption values are well compatible with the absorption coefficients of baroque woodcarvings measured in a reverberant chamber.[28]

In order to understand this phenomenon better and improve the accuracy of the estimation a preliminary investigation was carried out using scale model testing in a 1:20 reverberant chamber. A 1/8 in. microphone (GRAS 40DP) with a flat frequency response (± 1 dB) up to 30 kHz was used as the receiver. A spark generator with adjustable energy discharge and air gap was used as the sound source. The measurements presented here were made in air with numerical corrections for absorption according to ISO 9613-1.[27] Given the above set-up the full scale frequency range was 125–1000 Hz.

TABLE III. Calculation of mean absorption coefficient α as a function of octave bands, using Sabine's formula and assuming the whole basilica as a single volume. α_{res} is assumed as the average absorption coefficient obtained by subtracting the contribution of the marble floor (having a surface of 12 600 m^2 and the absorption coefficients reported in Table II).

	Frequency (Hz)					
	125	250	500	1000	2000	4000
T_{30} (s)	13.6	12.5	10.9	8.9	6.9	4.5
A_{tot} (m^2)	5604	6125	7029	8558	11 142	16 982
A_{air} (m^2)	106	315	656	1122	2 378	7 136
$A_{tot}-A_{air}$ (m^2)	5498	5810	6373	7436	8 764	9 846
α	0.07	0.08	0.08	0.10	0.11	0.13
α_{res}	0.08	0.09	0.10	0.11	0.13	0.15

TABLE IV. Summary of the results of the measurements of absorption coefficients carried out in 1:20 scale model reverberant chamber. Results report only relative variations compared to a flat sample of the same material used to reproduce the decorative patterns.

		Relative increment per octave band (Hz)			
Sample type	Surface ratio	125	250	500	1000
Fluted pillar	2:1	1.5	1.5	1.3	1.3
Simple coffered pattern	2:1	1.3	2.1	2.0	1.7
Decoration	n.a.	1.5	1.6	1.9	2.0

Three gypsum models were made, two (approximately) reproducing decorative patterns typically found in churches and the third reproducing a simplified coffered pattern. To account for the different acoustic behavior of materials at high frequencies all the absorption measurements were expressed in relative terms by comparison with a flat sample of the same material. Curved diffusers made of polypropylene sheets were used in the chamber model to ensure a reasonably diffuse sound field in all the conditions, and consequently ensure that the observed variations in reverberation time could be attributed to differences in sound absorption. The measurements show (Table IV) that the absorption coefficients were increased by a minimum of 30% up to 50% at 125 Hz, and from a minimum of 30% up to 100% at 1 kHz, doubling the absorption of the flat surface. Given the relative simplification adopted to model the samples, those results were used as floor values, allowing greater increases when dealing with more richly decorated surfaces.

The previous results suggested assigning to coffered vaults, moderately decorated surfaces (domes and arches), and sculptures the absorption coefficients given in Table II. However, the absorption coefficients of the largest surface (about 30 000 m^2, 40% of the total surface), covered by richly decorated marble and stuccos, were finally determined by iteration, during the calibration of the GA model (see below), in order to have the best match between measured and predicted values. The resulting absorption coefficients were those given in the last line of Table II, showing an increase of 50%–75% with respect to the reference value, in good agreement with both the findings of the scale model measurements and the values derived from measurements in other churches.

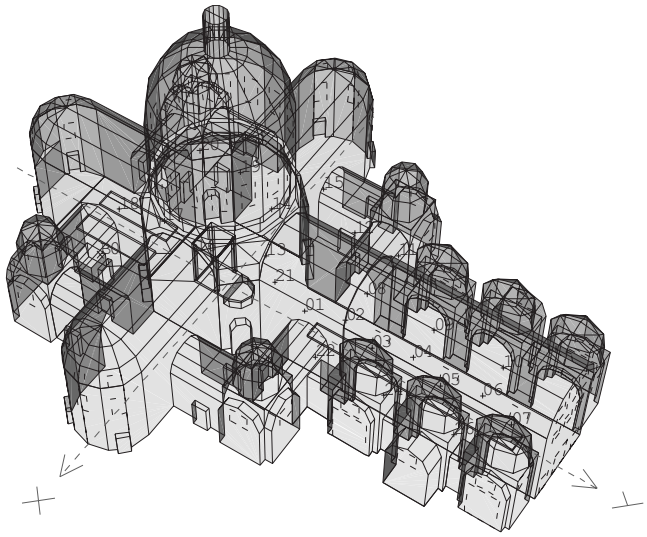

FIG. 8. GA model used to simulate the acoustics of the basilica.

B. GA model

Taking into account some geometrical measurements carried out in the field, combined with architectural drawings available in literature, a simplified 3D model was realized using about 1500 planes (Fig. 8). Source and receiver placement were arranged in order to correspond to actual positions used during the acoustic survey. As the late-part ray-tracing algorithm[17] can be considered as a Monte Carlo approximation to the exact solution and, consequently, it suffers from run-to-run fluctuations, which can be reduced by using a large number of rays, 1×10^6 rays were used in this case, while the truncation time was assumed to be equal to 14 s, slightly above the longest measured T_{30}. In addition, final results were given as averages over five different predictions for each source position together with the corresponding 95% confidence intervals (Table V). The latter were very small (corresponding to about 1.2% of the predicted value), suggesting that number of rays and truncation time were properly chosen.

Different surface treatments were accurately simulated taking advantage of photographs and field observations. Absorption coefficients were assigned as explained in Sec. IV A, while scattering coefficients were assigned taking into account the dimension of surface irregularities compared to

TABLE V. Summary of the octave-band values of reverberation time measured and predicted using different formulas, GA model, and SA model of coupled spaces. GA values are given with the corresponding confidence interval resulting from run-to-run fluctuations.

	Reverberation time (T_{30}) per octave band (Hz)					
	125	250	500	1000	2000	4000
Measured	13.6	12.5	10.9	8.9	6.9	4.5
Sabine's formula (single room)	11.4	10.9	9.8	8.0	6.5	4.1
Eyring's formula (single room)	11.8	11.4	10.1	8.2	6.7	4.2
GA model	13.4 ± 0.21	12.6 ± 0.15	11.0 ± 0.13	8.9 ± 0.11	7.1 ± 0.08	4.4 ± 0.04
SA model Sabine (coupled)	13.5	12.7	11.3	9.2	7.3	4.4
SA model Eyring (coupled)	13.0	12.2	10.9	8.8	6.9	4.2

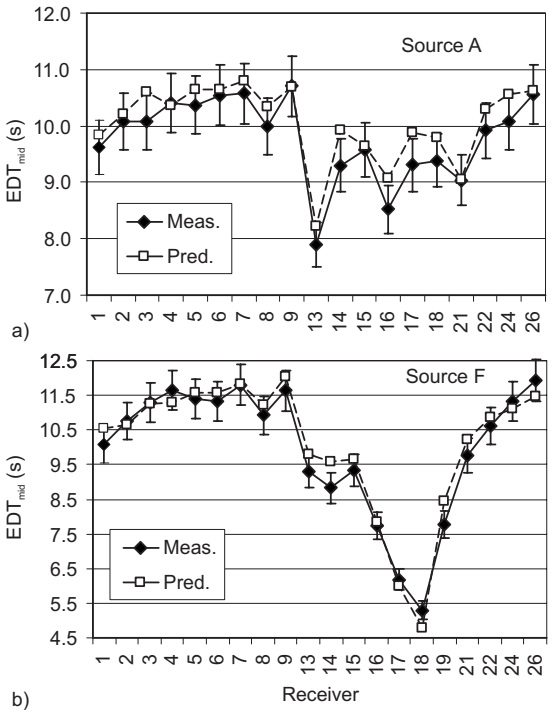

FIG. 9. Plot of EDT averaged over 500 and 1000 Hz octave bands measured (—) at different receivers compared with corresponding values predicted with GA model (---). Error bars correspond to JND for given parameter (equal to 5% of measured value).

wavelength. Flat or scarcely decorated surfaces were assigned scattering coefficients varying from 0.12 at 125 Hz to 0.17 at 4 kHz, including a linear increase of 0.01 to account for frequency dependence. Shallow decorated surfaces were assigned higher scattering coefficients varying linearly from 0.20 at 125 Hz to 0.40 at 4 kHz. Finally, pews, sculptures, and coffered vaults were assigned scattering coefficients varying from 0.30 at 125 Hz up to 0.80 at 4 kHz.

The prediction accuracy was estimated by calculating average rms errors over each source-receiver combination and expressing it in terms of just noticeable difference (JND), corresponding for T_{30} and EDT to 5% of the measured value.[29] With reference to source A the measured T_{30} were matched almost perfectly, with an octave-band error below one-half JND from 125 Hz to 4 kHz. The resulting mid-frequency values of EDT [Fig. 9(a)] were also predicted with good accuracy (average error of 0.9 JND), as well as other acoustic parameters not discussed here, such as strength (average rms error of 0.6 dB) and clarity (average rms error of 1.5 dB), suggesting good reliability of the model. The comparison between measured and predicted values with reference to source F [Fig. 9(b)] was carried out using the same settings, leading to the following average errors (at mid-frequency) of 1.0 JND for T_{30} and 0.8 JND for EDT. Other parameters were also predicted with reasonable accuracy with an average rms error of 0.4 dB for strength and 2.0 dB for clarity.

The GA model finally predicted T_{30} and EDT with good accuracy and showed that T_{30} values calculated with either Sabine's or Eyring's formula assuming the whole church as a single large room and using the same absorption coefficients were lower (Table V). As the basilica is the combination of different volumes, Sabine's formula was expected to fail. However, contradicting Shankland and Shankland's hypothesis,[5] the underprediction of T_{30} proved that the coupled-space model required absorption coefficients greater than those resulting from application of the above formulas to the whole volume.

Bayesian analysis applied to predicted IRs located in the choir showed results in agreement with those measured, with only slightly smaller values, indicating that at 1 kHz T_1 for this subspace is about 2.8 s (average $\tau_1=0.018$), while T_2 is 8.2 s (average $\tau_2=0.16$). When the source was in the crossing the steep initial decay was difficult to detect, probably because much of the radiated energy propagated to the adjacent subspaces, so that it was rapidly overtaken by the coupled-system decay.

C. SA model

The final comparison was carried out by applying a model of coupled subspaces, i.e., dividing the whole interior volume into subspaces and applying the classical diffuse-field equations to each of them, assuming they are connected by apertures through which acoustic energy may be exchanged.

In order to mathematically represent the decay of sound in acoustically coupled spaces, the nonstationary processes of sound energy decay are considered, following either steady state or impulse excitations. The sound energy decay in the whole interior, divided into m acoustical subspaces, is described by a system of m sound energy balance equations[16]

$$V_i(d\varepsilon_i/dt) = -cA_i\varepsilon_i/4 + \sum_j cS_{ij}(\varepsilon_j - \varepsilon_i)/4, \quad (1)$$

where $i=1,\ldots,m$, c is the sound speed, ε_i denotes the average sound energy density in the ith subspace, V_i is the volume of the ith subspace, and A_i is the equivalent absorption area of the ith subspace calculated according to Sabine's model as $S_i\bar{\alpha}_i+4mV_i$, where S_i and $\bar{\alpha}_i$ are, respectively, the total surface area and the geometrically averaged absorption coefficient of the ith subspace and $4mV_i$ is the propagation loss due to air. The coupling area between subspace i and adjacent subspace j is denoted $S_{i,j}$.

Following the approach of Summers *et al.*,[16] the above equation may be modified to account for using Eyring absorption exponent α_i' instead of $\bar{\alpha}_i$. Defining η_i as the ratio $\alpha_i'/\bar{\alpha}_i$, Eq. (1) may be modified by multiplying A_i by η_i.

The resulting system of linear differential equation (1) can be presented in matrix form and solved by finding the corresponding eigenvalues δ_i and eigenvectors ε_0^i (see Ref. 16 for mathematical details), and finally determining the constant terms from initial conditions.

One of the main issues to be addressed when solving coupled-volume problems by means of statistical analysis is the general validity of the basic assumption of statistical models. This means that inside each subspace the sound field must be reasonably diffuse. Furthermore, it is known that SA models are most accurate when applied to systems that are not strongly coupled. In strongly coupled systems the acous-

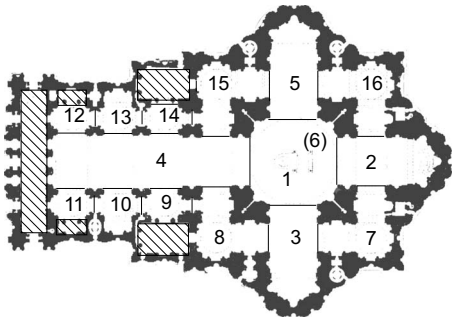

FIG. 10. Subdivision of the basilica into 16 subspaces. Subspace 6 refers to the dome. Dashed areas correspond to subspaces separated by doors and not included in the model.

tic energy is equally distributed, while in weakly coupled systems the subsystems behave as if they were isolated. Intermediate cases may be described by a theory that accounts for the exchange of energy between the spaces. A criterion to define how coupled two spaces are is therefore highly necessary. According to Kuttruff[2] SA models are applicable when energy lost via coupling is not substantially larger than the energy lost via absorption. Cremer and Muller[1] provided a coupling factor defined as

$$k_i = \frac{S_{ij}}{A_i + S_{ij}}, \tag{2}$$

giving strong coupling when $k_i \approx 1$ and weak coupling when $k_i \approx 0$. Further causes of discrepancies may appear as the subspaces become more strongly coupled. In fact, large apertures cause anisotropy in the sound field due to the establishment of a net flow of energy and alteration of the free-path distribution.[16]

Taking into account that surface decorations and the geometry ensure a high level of diffusion inside each subspace, the second most important issue to be evaluated is the coupling level, which should not be too high to prevent the above mentioned problems. In order to satisfy this condition the whole volume of the church was subdivided into 16 subspaces (Fig. 10) and, according to Eq. (1), for each subspace volume, total surface area, total absorption, and coupling area were calculated. Calculations were performed by using the same geometrical information and absorption coefficients derived from the GA model. The coupling factor, calculated according to Eq. (2), varied between 0.34 and 0.63, reasonably below the limit of 1, which corresponds to perfect coupling and potential lack of accuracy in the model solution.

According to the approach of Summers *et al.*,[16] when the sound source was located in room i, a fraction of its radiated power P was assumed to directly propagate into adjacent sub-rooms according to the fraction of the total solid angle subtended by the coupling surface S_{ij} as viewed from the source. Assuming a point source located close to the actual source positions the fraction was calculated by numerical integration for subspaces 1 (which radiates toward subspaces 2, 3, 4, 5, and 6) and 2 (which radiates toward subspaces 1, 4, 7, and 16).

In addition, Ref. 16 reports that one problem that is strictly related to complex spaces with multiple connections is a non-diffuse transfer of energy, which determines radiation of sound energy through the coupling aperture that is distinct from the energy density of the reverberant field of the room into which it radiates. In this way reverberant energy may be directly transferred between rooms that are not adjacent, depending on the radiation shape factor between the two apertures. In the present case, this correction is particularly useful when the sound source is located in the choir, as a significant part of its reverberant energy is likely to be transferred to the subspaces connected to the crossing without being reflected. This fraction was given by radiation shape factors that were calculated (according to Eq. 21 in Ref. 16) using numerical solving based on a contour double integral formula. As a consequence the energy fractions directly radiated from subspace 2 to subspaces 3, 4, 5, and 6 are, respectively, 0.116, 0.121, 0.116, and 0.101. The fraction directed toward subspace 4 was reduced to 0.08 to take into account the masking effect of Bernini's baldachin. The corresponding coupling surfaces were consequently rearranged according to Eq. (22) in Ref. 16.

Surfaces were assigned the same absorption coefficients used in the GA model and calculations were performed by using both Sabine's and Eyring's absorption exponents. Results derived from the application of the SA model were in good agreement with those derived from the GA model. In fact, as reported in Table V, it can be observed that values calculated with Sabine's formula are best matched with low frequency values (where mean absorption is lower), while those calculated with Eyring's formula are best matched with medium and high frequencies. In all the cases the reverberation times resulting from the coupled-volume model are longer than the corresponding values calculated assuming the whole space as a single room.

Even though the time constants of the 16 exponentials contributing to each decay curve are well known, in order to compare the results predicted by the SA model with those derived from Bayesian estimation, the latter algorithm was applied to determine the initial decay times corresponding to each subspace, when the sound source is inside the same space. Calculations were carried out at the frequency of 1 kHz and taking into account decays obtained using Eyring's correction. The results show that both in the crossing (where $T_1 = 1.8$ s) and in the choir (where $T_1 = 2.8$ s), predictions are in quite good agreement with results deriving from measurements.

When the source was in the crossing [Fig. 11(a)] much of the radiated energy propagated to the adjacent subspaces, consequently the steep initial decay is not as evident as in other subspaces, being rapidly overtaken by the coupled-system reverberation. When the receiver was located in the choir or in the nave the initial decay is slower (as a consequence of the energy exchange between adjacent subspaces) and rapidly fades into the coupled-system reverberation. When the source was in the choir [Fig. 11(b)] the initial decay appears clearly when the receiver was in the same subspace, while in the crossing the shorter initial decay is barely perceptible. When the receiver was in the nave, the initial energy is negligible, so the initial slope is near zero.

Even though the decay curves show a non-linear behav-

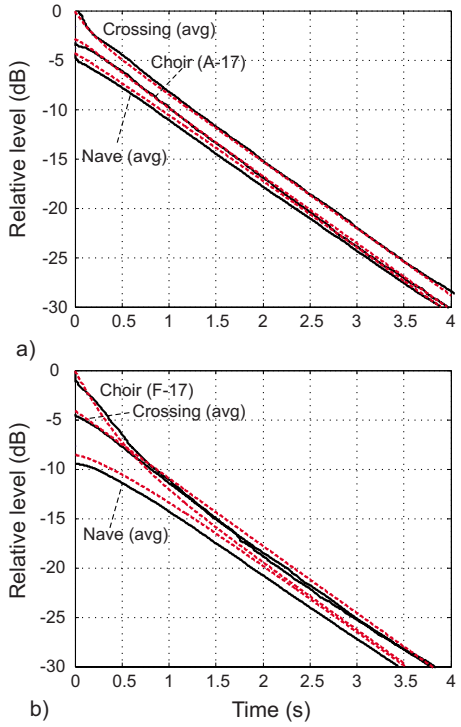

FIG. 11. (Color online) Comparison between early decay curves predicted using the SA model (- - -) and those obtained by averaging measured values at points representative of the same source-receiver combination (——). (a) Sound source located in the crossing in front of the altar. (b) Sound source located in the choir.

ior (suggesting that T_{30} and EDT should be treated carefully), a final comparison between the subspace averages of the above mentioned parameters and those predicted by the GA and SA models at the same frequency shows (Fig. 12) good agreement (with differences generally below 5%), confirming the accuracy of both the prediction-models.

A comparison between values calculated with and without solid angle correction for direct radiation and non-diffuse energy transfer proved that, as suggested by Summers *et al.*,[16] their inclusion is useful in giving accurate estimation of the initial decay, leading to better EDT predictions.

Given the good accuracy provided by the simple SA model of coupled volumes it is particularly interesting to analyze sound behavior in subspaces where, due to time limitations, no sound sources were placed during the survey. A sound source located in the diagonal chapel (subspace 8) would determine, in the same subspace, a $T_1=2.3$ s with the coupled-volume reverberation ($T_2=8.8$ s) appearing more than 15 dB after the direct sound. This implies that EDT (equal to 2.9 s) is strongly influenced by T_1, while T_{30} becomes less significant as the decay curve within the measuring interval is markedly non-linear. Similarly, in one of the side chapels (subspace 10), $T_1=1.7$ s, and T_2 appears after 20 dB, so EDT=2.5 s, while T_{30} is not significant. The latter results suggest that the acoustics of the secondary volumes of the basilica, frequently used (even today) for daily celebrations, may provide better conditions for speech intelligibility.[30]

All the above considerations refer to the unoccupied conditions. A large congregation would add absorption, reducing the coupling factor [see Eq. (2)] and finally leading to a weaker coupling. This means that energy exchange between volumes would be reduced, emphasizing differences among them. As this configuration is actually the most important for the listener, a simple calculation was made using the SA model and assuming a seated audience (1.5 person/m^2, $\alpha=0.99$ at 1 kHz) distributed over 70% of the floor area of the four braces and the crossing. Results show that the coupled-system reverberation at 1 kHz would be lowered to 6.1 s. EDT in the nave would be 5.5 s with the source on the altar, and 6.6 s with the source in the choir. A sound source located in the crossing and then in the choir would determine in each subspace, respectively, EDTs of 4.4 and 3.1 s.

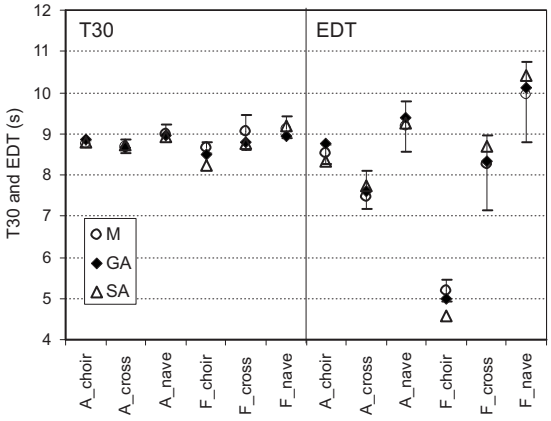

FIG. 12. Plot of average values of T_{30} and EDT measured at 1 kHz octave band in different subspaces and with different source positions compared to values predicted with both GA and SA models. Error bars represent variations between measured values.

V. CONCLUSIONS

The analysis of experimental data showed that reverberation times measured in St. Peter's Basilica are actually shorter than generally observed in churches of even smaller dimensions. In addition, significant differences appeared among EDT values, suggesting important acoustic differences between subspaces. Bayesian parameter estimation suggested that coupling effects actually take place and the analysis of the directional distribution of reflected energy allowed visualizing these effects.

The application of GA and SA models showed that St. Peter's Basilica actually behaves as a system of coupled volumes in which the acoustic conditions may significantly vary from subspace to subspace, according to source and receiver placements. Both models show that the resulting reverberation time is longer than that predicted using either Sabine's or Eyring's formula assuming the whole space as a single room volume. This implies that, given the substantial similarity of the surface treatment in the main nave and in the side chapels, in order to obtain the measured reverberation time the above mentioned surfaces should have increased absorption properties, mostly depending on the increased exposed surface due to the high degree of decoration, contradicting Shankland and Shankland's hypothesis[5] that the lower reverberation might result from coupling. Conversely,

coupling effects explain the dependence of reverberation on source and receiver position, leading to sound perception, which may be quite different from point to point, demonstrating how this building is capable of sounding not only like a big cathedral during solemn celebrations but also like a small parish church during daily services celebrated in the secondary volumes. Further investigations are needed in order to better clarify the mechanism of increased absorption shown by decorated surfaces.

ACKNOWLEDGMENTS

The author would like to thank His Eminence Cardinal Angelo Comastri, President of the Fabric of St. Peter's, Archpriest of St. Peter's Basilica in the Vatican for granting access to the church. He is also grateful to Professor Ettore Cirillo for encouraging and supporting this research, to Michele D'Alba for his kind cooperation in organizing and carrying out the survey, and to Rendell Torres and Jason Summers for their help in reviewing the paper.

[1]L. Cremer and H. A. Muller, *Principles and Applications of Room Acoustics* (Applied Science, London, 1982), Vol. **1**.
[2]H. Kuttruff, *Room Acoustics*, 3rd ed. (E & FN Spon, London, 1991).
[3]V. O. Knudsen, "The effect of form on the reverberation of sound in rooms," J. Acoust. Soc. Am. **3**, 314 (1932).
[4]A. C. Raes and G. Sacerdote, "Measurement of the acoustical properties of two Roman basilicas," J. Acoust. Soc. Am. **25**, 954–961 (1953).
[5]R. S. Shankland and H. K. Shankland, "Acoustics of St. Peter's and Patriarchal Basilicas in Rome," J. Acoust. Soc. Am. **50**, 389–395 (1971).
[6]E. Cirillo and F. Martellotta, *Worship, Acoustics, and Architecture* (Multiscience, Brentwood, UK, 2006).
[7]A. Trochidis, "Reverberation time of Byzantine churches of Thessaloniki," Acustica **51**, 299–301 (1982).
[8]T. H. Lewers and J. S. Anderson, "Some acoustical properties of St. Paul's Cathedral, London," J. Sound Vib. **92**, 285–297 (1984).
[9]J. S. Anderson and M. Bratos-Anderson, "Acoustic coupling effects in St. Paul's Cathedral, London," J. Sound Vib. **236**, 209–225 (2000).
[10]C. F. Eyring, "Reverberation time measurements in coupled rooms," J. Acoust. Soc. Am. **3**, 181–206 (1931).
[11]B. Harrison and G. Madaras, "Computer modeling and prediction in the design of coupled volumes for a 1000-seat concert hall at Goshen College, Indiana," J. Acoust. Soc. Am. **109**, 2388(A) (2001).
[12]N. Xiang and P. M. Goggans, "Evaluation of decay times in coupled spaces: Bayesian parameter estimation," J. Acoust. Soc. Am. **110**, 1415–1424 (2001).
[13]N. Xiang and P. M. Goggans, "Evaluation of decay times in coupled spaces: Bayesian decay model selection," J. Acoust. Soc. Am. **113**, 2685–2697 (2003).
[14]N. Xiang, P. M. Goggans, T. Jasa, and M. Kleiner, "Evaluation of decay times in coupled spaces: Reliability analysis of Bayesian decay time estimation," J. Acoust. Soc. Am. **117**, 3707–3715 (2005).
[15]N. Xiang and T. Jasa, "Evaluation of decay times in coupled spaces: An efficient search algorithm within the Bayesian framework," J. Acoust. Soc. Am. **120**, 3744–3749 (2006).
[16]J. E. Summers, R. R. Torres, and Y. Shimizu, "Statistical-acoustics models of energy decay in systems of coupled rooms and their relation to geometrical acoustics," J. Acoust. Soc. Am. **116**, 958–969 (2004).
[17]J. E. Summers, R. R. Torres, Y. Shimizu, and B. I. Dalenback, "Adapting a randomized beam-axis-tracing algorithm to modelling of coupled rooms via late-part ray tracing," J. Acoust. Soc. Am. **118**, 1491–1502 (2005).
[18]S. Müller and P. Massarani, "Transfer-function measurement with sweeps," J. Audio Eng. Soc. **49**, 443–471 (2001).
[19]ISO-3382, "Acoustics—Measurement of the reverberation time of rooms with reference to other acoustical parameters," ISO, Geneva, Switzerland, 1997.
[20]F. Martellotta, E. Cirillo, A. Carbonari, and P. Ricciardi, "Guidelines for acoustical measurements in churches," Appl. Acoust. **70**, 378–388 (2009).
[21]E. Cirillo and F. Martellotta, "Sound propagation and energy relations in churches," J. Acoust. Soc. Am. **118**, 232–248 (2005).
[22]F. Martellotta, "A multi-rate decay model to predict energy-based acoustic parameters in churches," J. Acoust. Soc. Am. **125**, 1281–1284 (2009).
[23]B. N. Gover, J. G. Ryan, and M. R. Stinson, "Measurements of directional properties of reverberant sound fields in rooms using a spherical microphone array," J. Acoust. Soc. Am. **116**, 2138–2148 (2004).
[24]M. Vorländer, *Auralization* (Springer-Verlag, Berlin, 2008).
[25]J. Meyer, *Kirchenakustik* (Verlag Erwin Bochinsky, Frankfurt am Main, Germany, 2003).
[26]T. J. Cox and P. D'Antonio, *Acoustic Absorbers and Diffusers* (Spon, New York, 2004).
[27]ISO 9613-1, "Acoustics—Attenuation of sound during propagation outdoors—Part 1: Calculation of the absorption of sound by the atmosphere," ISO, Geneva, Switzerland, 1993.
[28]A. P. O. Carvalho, M. Lencastre, and V. Desarnaulds, "Sound absorption of 18th-century baroque woodcarving in churches," Proceedings of the Inter-Noise 2002, Dearborn, MI, August (2002).
[29]I. Bork, "A comparison of room simulation software—The 2nd round robin on room acoustical computer simulation," Acust. Acta Acust. **86**, 943–956 (2000).
[30]B. Yegnanarayana and B. S. Ramakrishna, "Intelligibility of speech under nonexponential decay conditions," J. Acoust. Soc. Am. **58**, 853–857 (1975).